ORIGINAL PAPER

Comparison of characteristics of aerosol during rainy weather and cold air-dust weather in Guangzhou in late March 2012

Huizhong Chen · Dui Wu · Jianzhen Yu

Abstract Using the data on aerosol observed hourly by Marga ADI 2080 and Grimm 180, we compared the characteristics of aerosol during rainy weather and cold air-dust weather in Guangzhou in late March 2012. The mass concentration of aerosol appeared distinct between the two weather processes. During rainy weather, the mass concentration of PM and total water-soluble components decreased obviously. During cold air-dust weather, the cleaning effect of cold air occurred much more suddenly and about a half day earlier than the dust effect. As a result, the mass concentration of PM and total water-soluble components first dropped dramatically to a below-normal level and then rose gradually to an above-normal level. The ratio of $PM_{2.5}/PM_{10}$ and PM_1/PM_{10} decreased, suggesting that dust-storm weather mainly brought in coarse particles. The proportion of Ca^{2+} in the total water-soluble components significantly increased to as high as 50 % because of the effect of dust weather. We further analysed the ionic equilibrium during rainy and cold air-dust weather, and compared it with that during hazy weather during the same period. The aerosol during rainy weather was slightly acidic, whereas that during hazy weather and cold air-dust weather was obviously alkaline, with that during cold air-dust weather being significantly more alkaline. Most of the anions, including SO_4^{2-} and NO_3^-, were neutralised by NH_4^+ during rainy and hazy weather, and by Ca^{2+} during cold air-dust weather.

1 Introduction

Aerosol plays an important role in the change in global climate system and the formation of regional air pollutants. On the one hand, aerosol influences radiation flux and therefore affects the surface temperature on earth by absorbing and scattering short-wave and longwave radiation (Deluisi et al. 1976; Coakley et al. 1983; Jayaraman 2001; Wendisch et al. 2002; Kim et al. 2005; Presto et al. 2005; Takemura et al. 2005). On the other hand, as an important cloud condensation nucleus, aerosol participates in the formation of cloud droplets, and therefore changes the physical structure of clouds as well as increases cloud and rainfall amount (Rotstayn and Lohmann 2002; Lau and Kim 2006; Jin and Shepherd 2008; Gautam et al. 2009; Rotstayn et al. 2012). Moreover, aerosol is a major air pollutant that can obviously decrease visibility and lead to hazy weather (Jinhuan and Liquan 2000; Lee and Sequeira 2002; Wu 2003; Chow et al. 2004; Wu et al. 2006a; Li et al. 2008a, b). Inhalable aerosol particles can enter the human respiratory system and significantly harm human health (Avol et al. 1979; Raizenne et al. 1989; Raizenne 1996; Li et al. 2002; Pöschl 2005; Kennedy 2007). Since the occurrence of worldwide industrialisation and urbanisation, the amount of aerosol in the environment has increased, resulting in climate changes and worsening air pollution (Dockery et al. 1992; Thurston et al. 1994; Volkamer et al. 2006). Therefore, numerous studies have focused on identifying the physical and chemical properties of aerosol.

The characteristics of aerosol are closely related to weather conditions. For example, rain is one of the main methods of clearing aerosol in the air through the wet removal process (Garland 1978; Hales 1978; Flossmann et al. 1985). Aerosols collide with and are captured by rain droplets, and are thereby washed away by

H. Chen
Dongguan Meteorological Bureau, Dongguan 523000, China

D. Wu (✉)
Institute of Technology on Atmospheric Environmental Safety and Pollution Control, Jinan University, Guangzhou 510632, China
e-mail: wudui@grmc.gov.cn

H. Chen · D. Wu
Institute of Tropical and Marine Meteorology, CMA, Guangzhou 510080, China

J. Yu
Department of Chemistry, Hong Kong University of Science and Technology, Clear Water Bay, Hong Kong, China

rainfall. As a result, the size distribution of aerosol changes. This wet removal process by rainfall is highly important and is included in many models of aerosol-scavenging coefficient (Mircea et al. 2000; Chate and Pranesha 2004; Zhang et al. 2004; Zhao and Zheng 2006). Dusty and sand-storm weather is also a major natural source of aerosol. In the source areas of dust, a large amount of crustal material is directly brought to the atmosphere, which leads to a dramatic increase in particle concentration (Rogge et al. 1993; Tegen and Fung 1995; Prospero et al. 2002). In some cases, the mass concentration of particles exceeds the national standard by four to five times (Qiu 2004; Zhi et al. 2007; Gu et al. 2009). Apart from having a local impact, dust storms can transport particles to down-wind areas and influence the aerosol characteristics there. During long-range transport, the composition of dust aerosol could change by mixing with the aerosol particles along the way (Wang et al. 2007). Therefore, the long-range impact of dust aerosol depends on the transport pathway and might have varying effects on different destinations.

Guangzhou, a mega city in the Pearl River Delta area, witnessed an increase in aerosol pollutants in recent years (Wu 2003; Wu et al. 2006a; Li et al. 2008a, b). In Guangzhou, aerosol pollutants are mainly caused by fine particles (Wu et al. 2006b; Wu et al 2009), and the main water-soluble components are anions such as SO_4^{2-} and NO_3^-, and cations such as NH_4^+ and Na^+ (Xia et al. 2009). On the synoptic scale, various weather processes influence the properties of aerosol in Guangzhou. For example, in late March 2012, Guangzhou experienced rainy weather and a dust storm transported from northern China. In this paper, we discuss the characteristics of aerosol during this period to compare the impact of various weather processes on aerosol properties under a background of stable large-scale circulation.

Many studies have paid attention to the wet removal process of aerosol during rainy weather (e.g., Deng et al. 2012; Kang et al. 2009). Dust-storm weather usually occurs in northern regions in China, but can transport a long way and influence southern China. Previous studies have analysed the dust-storm effect on southern China regions. For example, Fang et al. (1999) studied the dust aerosol transported a long way from northern China to Hong Kong in May 1996, and pointed out the high Ca and Cl contents in soil samples. High Ca content suggests that the source of the aerosol is northern Chinese crustal material, and high Cl content indicates that the aerosol was transported by sea (East China Sea in this case). Shen et al. (2012) analysed the dust storm transported from Mongolia to Guangzhou in April 2009 and suggested that the mass concentration of PM_{10} obviously rose along with various water-soluble components, but the total proportion of SO_4^{2-}, NO_3^- and NH_4^+ remained stable (~82 %). These previous studies explored the characteristics of aerosol during dusty weather, but their observed data were inconclusive. During rainy and dusty weather affecting Guangzhou in late March 2012, we observed aerosol data on an hourly basis.

Such a finely scaled observation guarantees the quality of data and provides a good opportunity to examine the characteristics of aerosol over a continuous period of time.

This paper is organised as follows. Data and methods are described in Section 2. In Section 3, we examine the variations of aerosol components and weather variables in Guangzhou in late March 2010. In Section 4, we compare PM and water-soluble components in different weather processes. Then, in Section 5, we explore the characteristics of ionic equilibrium in different weather processes before presenting conclusions in Section 6.

2 Data

We use Marga ADI 2080 and Grimm 180 analysers to identify the water-soluble components and PM concentration of aerosol particles. The Marga ADI 2080 is an online analyser that measures specific aerosols and gases in ambient air. The analyser is composed of two boxes: a collection box and an analyser box. Air is drawn through the sampling system in the box, and then the inorganic gases and aerosol particles are absorbed and collected into separate absorption liquids. Then, the syringe of the analyser changes direction and the inorganic compounds in the gases and aerosols are determined by ion chromatography. Thus, we can obtain continuous data on water-soluble components. Then, Grimm 180 can measure PM concentration in 30 channels. This analyser can determine the concentration based on intensity and frequency of the received light because the aerosols would scatter the laser.

Compared with traditional sampling, the Marga instrument has high time resolution and information continuity, but the results exhibit certain differences. The correlation between these two methods is shown in Table 1 (Goodwin et al. 2009; Cowen et al. 2011), and the results were from the United States Environmental Protection Agency (US EPA). Table 1 shows that SO_4^{2-} and NH_4^+ have high correlation except NO_3^-. The results of the two tests also show differences. On

Table 1 Correlation between MARGA and sampling method

	US EPA report (MARGA 1)			US EPA report (MARGA 2)		
	SO_4^{2-}	NH_4^+	NO_3^-	SO_4^{2-}	NH_4^+	NO_3^-
2009						
Slope	0.92	0.82	0.48	0.87	0.85	0.40
Intercept	0.68	0.08	0.19	0.63	0.21	0.25
R^2	0.91	0.67	0.24	0.89	0.68	0.19
2011						
Slope	1.02	1.02	2.48	0.986	0.993	1.73
Intercept	0.3	−0.23	−1.05	0.22	−0.25	−0.05
R^2	0.995	0.959	0.774	0.994	0.958	0.76

the one hand, the correlation is lower in the first test than in the second one; on the other hand, the value of NO_3^- is higher in Marga. The US EPA considers the values of SO_4^{2-} and NH_4^+ to be accurate, whereas that of NO_3^- has some deviation. Thus, in this paper, we discuss only the trend of the aerosol components.

Aerosol sampling using Marga and Grimm 180 was performed from March 16th to 25th, 2012. The sampling station was in Guangzhou Nancun (113°21′E, 23°00′N), 150 km away from the sea and 141 m above sea level. The station was located at the heart of the Pearl River Delta Economic Zone, and can reflect the average environmental status of the Pearl River Delta.

3 Variations of different aerosol components and weather variables in Guangzhou in late March 2010

Figure 1 illustrates the time series of the mass concentration of $PM_{2.5}$ and various water-soluble components during the aforementioned period. The variations in concentrations of $PM_{2.5}$ and total water-soluble components appear highly similar, which suggests that the Marga data are synchronous with the observed mass concentration of $PM_{2.5}$. Their concentrations underwent the following stages: (1) from March 16th to 17th, the mass concentration of $PM_{2.5}$ presented a decreasing trend, gradually decreasing from 176.1 to 26.4 μg/m³ in 14 h from 16:00 on March 16th to 6:00 on the 17th; this decrease was accompanied by a decrease in the amount of total water-soluble components from 69.2 to 13.5 μg/m³. (2) During the period from March 18th to 22nd, the concentrations of $PM_{2.5}$ and the total water-soluble components concentration stayed at a relatively stable level of ~60 and ~20 μg/m³, respectively. Obvious fluctuation occurred in the middle of March 20th and 22nd. (3) On March 23rd, the $PM_{2.5}$ sharply decreased from 101.0 μg/m³ to 17.7 μg/m³ in 4 h from 10:00 on March 23rd to 14:00 on March 23rd, gradually rose to the level of 111.5 μg/m³, and then dropped to the stable level of ~60 μg/m³. The concentration of total water-soluble components

exhibited a similar variation. For each water-soluble component, the proportions will be discussed in detail later in this paper. We emphasise the dramatic increase of Ca^{2+} concentration after 8:00 on March 23rd, simultaneous with the sharp drop of $PM_{2.5}$ concentration. The concentration of Ca^{2+} rose from 1.8 to 20.7 μg/m³ from 8:00 on March 23rd to 14:00 on March 24th. The high Ca^{2+} concentration in the particles is a characteristic of northern Chinese crustal material (Liu 1985), indicating that Guangzhou was probably influenced by dusty weather from northern China during this period.

Figure 2 exhibits the variations of air pressure, relative humidity (RH) and temperature. Air pressure was stable at ~1174 hPa from March 16th to 19th, then slightly increased to ~1188 hPa from March 20th to early March 23rd. In the afternoon of March 23rd, the air pressure suddenly increased to as high as 1188 hPa and then oscillated at approximately 1181 hPa. For RH, from March 16th to 18th, it increased to 100 %, indicating that rainfall might happen. Rainfall would wash out aerosols, resulting in the decreasing concentration of $PM_{2.5}$ and the total water-soluble components. From March 19th to 22nd, RH stayed at a relative stable level of ~80 % on average. From the middle of March 23rd, RH decreased significantly to ~35 % on March 24th, and gradually increased thereafter. Temperature remained at an average level of ~24 °C and dramatically decreased to as low as 12.5 °C on the afternoon of March 23rd, and then gradually increased to ~20 °C. We noticed that all the analysed variations underwent a sudden change on March 23rd: air pressure increased, whereas RH decreased and temperature decreased. These sharp changes suggested approaching dry and cold air, which could be indicated by the surface weather map on March 23rd, showing an obvious high pressure centred north of Guangzhou and a strong northerly wind extended from northern China to Guangzhou (figure not shown). Compared with the data in Fig. 1, the concentrations of $PM_{2.5}$ and total water-soluble components decreased dramatically whereas Ca^{2+} obviously increased from March 23rd. This result indicates that, on the one hand, the occurrence of cold air could act as

Fig. 1 Time series of mass concentration of $PM_{2.5}$ (*line*) and various water-soluble components (*bar*) from March 16th to 25th, 2012. Unit: μg/m³
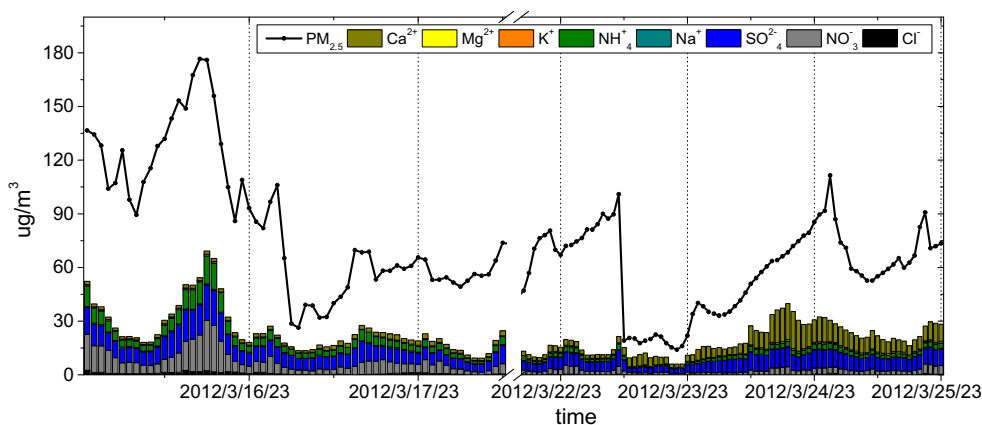
Fig. 2 Variations of air pressure (*green solid line*; unit: hPa), relative humidity (RH; *blue solid line*; unit: %) and temperature (*red solid line*; unit: °C) from March 16th to 25th, 2012. The *blue dotted line* denotes 100 % RH
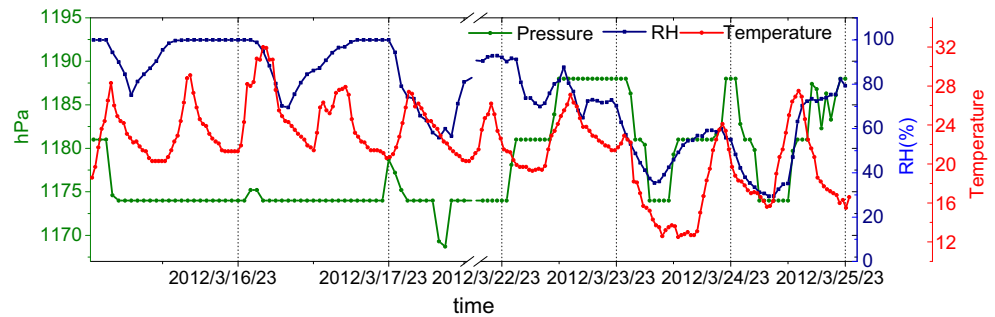

a cleaner to decrease aerosol pollutants; on the other hand, the intrusion of air from northern China might bring sand to Guangzhou from a dust-storm source in northern China. The cleaning effect seemed to emerge approximately half a day earlier than the dust-storm effect, and the cleaning effect was sudden whereas the dust effect was gradual.

To confirm the intrusion of cold air, we used a satellite image (Fig. 3) and analysed the 72-h backward trajectory diagram from March 22nd to 25th (Fig. 4), which can show the source of air reaching Guangzhou derived from 3 days previously. Figure 3 shows a NASA MODIS satellite image of South China, which was taken on March 23rd. The figure

illustrates that the banded cloud drove the cold air to south China, and behind the banded cloud were clouds similar to plumes, which would indicate an approaching sand storm. The air that reached Guangzhou on March 22nd was derived from the Bohai Sea area and transported southwestward through the sea surface east of China. From March 23rd to 25th, the air that reached Guangzhou was derived from the mainland areas north of Guangzhou (Fig. 4). The air was transported straight southward to Guangzhou. Therefore, Guangzhou was influenced by the air derived from northern China during the analysed period, and the air that reached Guangzhou from March 23rd to 25th was characterised by a straight southward trajectory.

Fig. 3 NASA MODIS imagery of South China on March 23, 2012
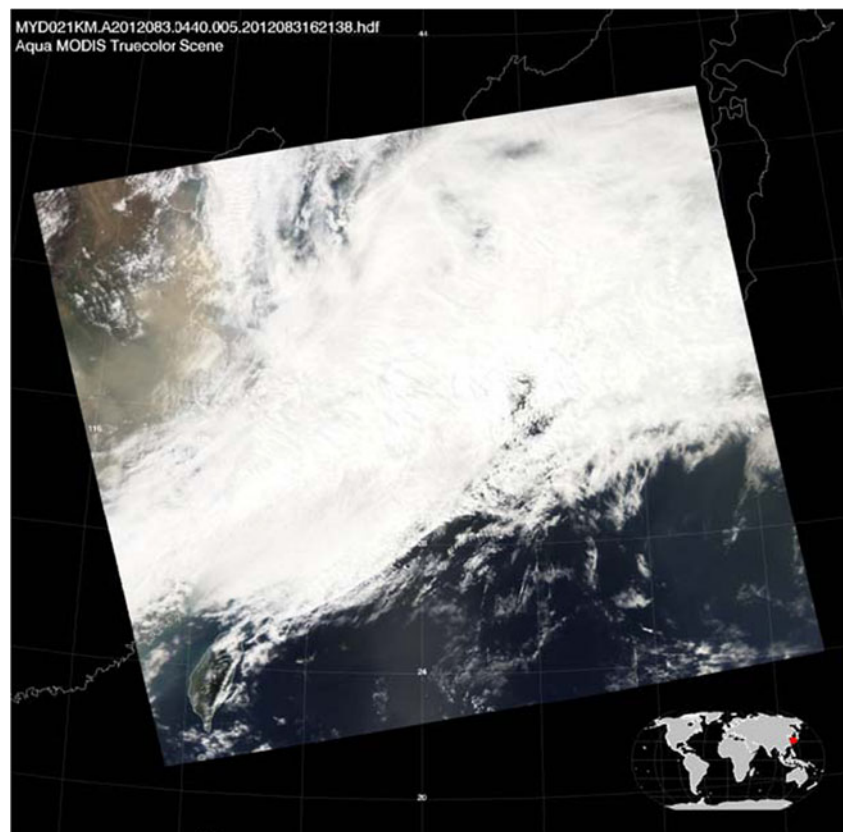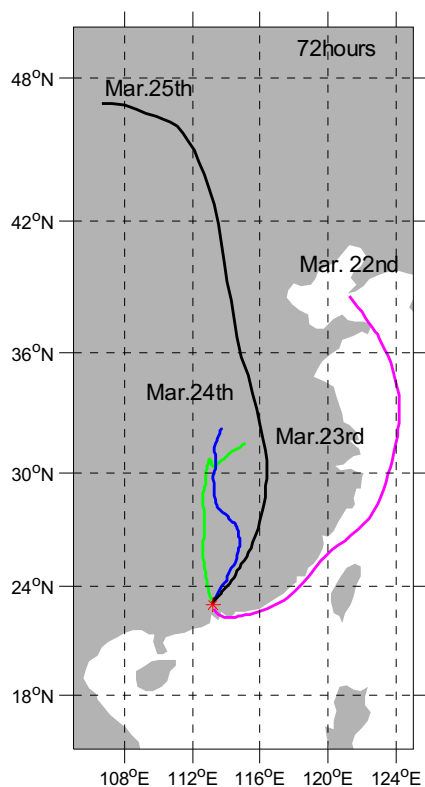
Fig. 4 72-h backward trajectory diagram of Guangzhou from March 22nd to 25th, 2012

4 Comparison of PM and water-soluble components in different weather processes

According to the preceding analyses, we divided the analysed period into three processes. Firstly, the period from March 16th to 17th is called the rainy period characterised by 100 % RH and decreased PM. Secondly, the period from March 18th to 22nd refers to the stable period characterised by variations that stayed relatively stable. Thirdly, the period from March 23rd to 25th is the cold air-dust weather period characterised by the intrusion of cold air (high pressure and low temperature) as well as a dramatic increase in Ca^{2+} concentration. Then, we explored in detail the variations of different air components during these three periods, focusing mainly on the rainy weather and the cold air-dust weather.
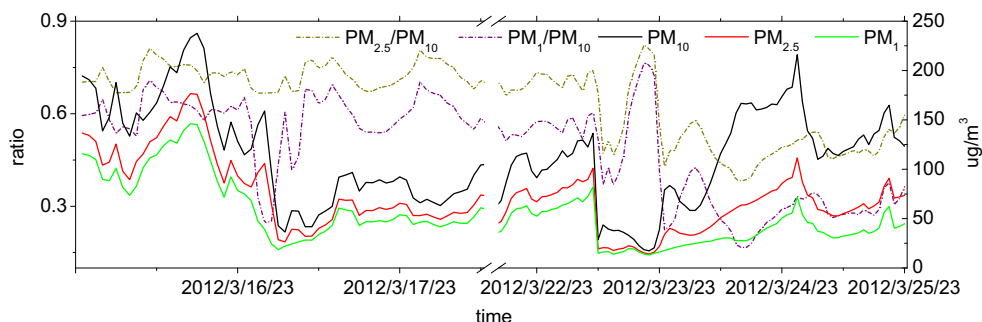
Figure 5 shows the time series of the concentrations of PM_{10}, $PM_{2.5}$ and PM_1 as well as the ratio of $PM_{2.5}/PM_{10}$ and PM_1/PM_{10}. During the rainy period from March to 17th, the concentration of PM decreased significantly because rainfall washed out aerosol particles. For example, the concentration of PM_{10} dropped from 237.7 to 36.5 $\mu g/m^3$. Meanwhile, the ratio of $PM_{2.5}/PM_{10}$ varied at approximately 0.7 and the PM_1/PM_{10} dropped. During the stable period from March 18th to 22nd, the concentrations and ratios of different PM varied around the stable levels. Then, during the cold air-dust weather period, accompanied by the arrival of cold air, the concentrations of all PM dropped obviously on March 23rd, and then rose to a higher level from March 24th with the dust effect, during which the concentrations of $PM_{2.5}$ and PM_1 were almost equal to those in the stable period, whereas the PM_{10} concentration (128.4 $\mu g/m^3$) was higher than that during the stable period (83.9 $\mu g/m^3$). As a result, the ratios of $PM_{2.5}/PM_{10}$ and PM_1/PM_{10} decreased significantly after the dust storm, from 0.71 and 0.57 to 0.42 and 0.22, respectively. Therefore, the dusty weather brought coarse particles to Guangzhou and caused a significant change in particle size distribution. During the dusty weather, the average level of PM_{10} was up to 171 $\mu g/m^3$, comparable with the level during previous dusty weather that affected southern China. For example, the concentrations of PM_{10} were 134 $\mu g/m^3$ and 231 $\mu g/m^3$ during the dusty weather in April 2009 (Lin et al. 2007) and March 2010 (Wu et al. 2011) in Guangzhou, and were 200 and 170 $\mu g/m^3$ during the dusty weather in April 2001 and March 2005 (Lin et al. 2007) in Taiwan. These results indicated that the average concentration of PM_{10} during the dust-storm weather analysed in this paper was at a reasonable level.

Figure 6 illustrates the variation of the proportions of various water-soluble components. The total proportion of Ca^{2+}, NH_4^+, SO_4^{2-}, and NO_3^- accounts for almost 95 %; thus, we mainly focused on these components. During the rainy period from March 16th to 17th, the total proportion of anions, including SO_4^{2-}, NO_3^- and Cl^-, exhibited a declining trend. The proportion of SO_4^{2-} rose and NO_3^- dropped, with the SO_4^{2-} and NO_3^- respectively accounting for ~38 and ~30 % before the rain, and ~47 and ~17 % after the rain. For the cations, the proportion of Ca^{2+} began to accumulate, whereas NH_4^+ and

Fig. 5 Time series of mass concentrations of PM_{10} (*black solid line*), $PM_{2.5}$ (*red solid line*), PM_1 (*green solid line*) (unit: $\mu g/m^3$) and ratio of $PM_{2.5}/PM_{10}$ (*grey dotted line*) and PM_1/PM_{10} (*purple dotted line*) from March 16th to 25th, 2012

Fig. 6 Variation of proportions of various water-soluble components from March 16th to 25th, 2012
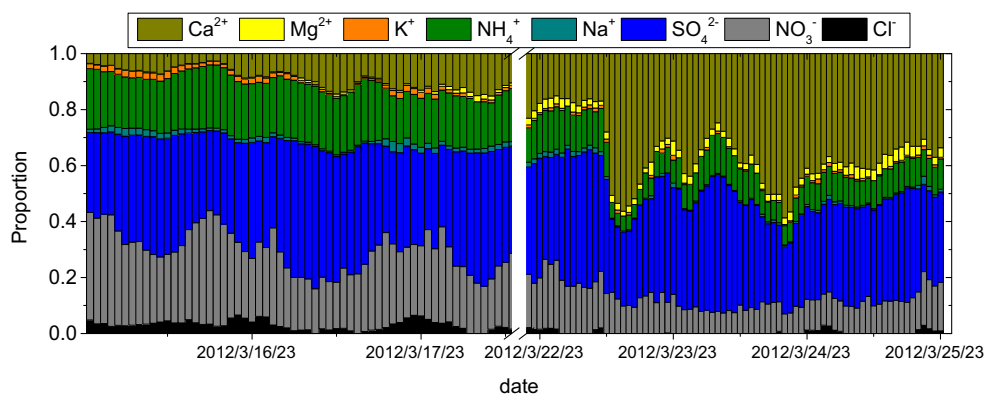
the other components had no significant change. Then, during the stable period from March 18th to 22nd, the total proportion of anions stayed at a stable level of ~70 %, with SO_4^{2-} accounting for ~50 % and NO_3^- accounting for ~20 %. For the cations, the concentration of Ca^{2+} and Mg^{2+} continued to accumulate while NH_4^+ and K^+ decreased. Ca^{2+} and Mg^{2+} are mainly derived from crustal materials that can be transported from northern to southern China. The accumulation of Ca^{2+} and Mg^{2+} is consistent with the prevailing northerly wind in Guangzhou during this period, which can be inferred from the southward trajectory shown in Fig. 4.

Finally, during the cold air-dust weather period, the structure of the water-soluble components changed significantly. The concentration of Ca^{2+} increased more than 10 times from 1.8 to 20.8 μg/m³ with the arrival of the cold air, and the Ca^{2+} suddenly became the main composite of the observed particles, reaching as high as ~50 % in the afternoon on March 23rd and at nighttime on March 24th. These two peak values exhibited the cold air intrusion and its dusty effect, respectively. Mg^{2+} also accumulated and exhibited an obvious increase during this period, again indicating the influence of dusty weather. Moreover, Na^+ and Cl^- showed a dramatic decrease during this period, with concentration proportion near zero. The reason is that Na^+ and Cl^- were mainly derived from sea salt aerosol in the more humid air, but the arrival of dry air from northern China greatly decreased the air humidity and the proportion of sea salt aerosol. Therefore, we can conclude that the intrusion of cold air and dust aerosols from northern China replaced the original air particles in Guangzhou and significantly changed the aerosol characteristics.

5 Characteristics of ionic equilibrium in different weather processes

The preceding analyses pointed out that two weather processes affected Guangzhou from March 16th to 25th: rainy weather and cold air-dust weather. We noticed another typical weather condition that occurred during this period: hazy weather occurred on March 22nd, characterised by average

relative humidity of 83.7 % and visibility of 6.21 km, which met the definition of haze (average relative humidity <90 % and visibility <10 km). Considering that haze is an important weather characteristic that influences Guangzhou, we compared the ionic equilibrium characteristics of aerosols during the hazy weather in addition to the rainy and cold air-dust weather during the analysed period.

Figure 7 illustrates the cation–anion scatter plots and their fitting lines for the three weather processes. Table 2 shows the Statistical parameters in different weather processes. As Li et al. (2008a, b) pointed out in a study on aerosols in Beijing, the relationship between the total cations and anions could be used to denote the acidity of the aerosol. The fitting linear slope of anion to cation can quantitatively estimate the acidity of the aerosol: a slope larger (smaller) than 1 indicates that the aerosol is acidic (alkaline), and a slope equal to 1 indicates that the aerosol is neutral. Figure 6 shows that the fitting lines for different weather processes exhibit obvious differences. The fitting slopes are 1.07 for rainy weather, 0.63 for hazy weather and 0.24 for cold air-dust weather. Therefore, the aerosol acidity was distinct for different
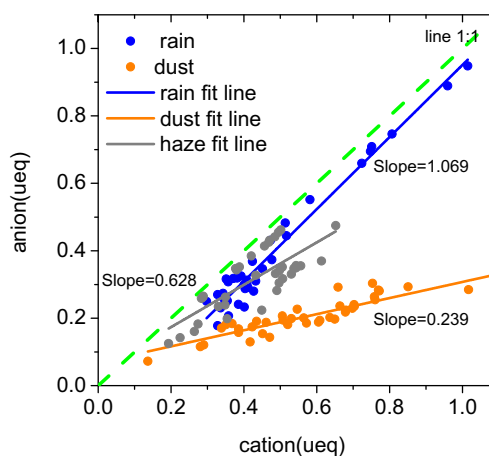
Fig. 7 Scatter plots of cation and anion and their fitting lines (anion to cation) in different weather processes: *blue* denotes rainy weather, *yellow* denotes dusty weather and *grey* denotes hazy weather. The *green dotted line* denotes the reference line with a slope of 1. The adjusted R^2, intercept, and slope for each fitting line are labelled nearby

Table 2 Statistical parameters in different weather processes

		Haze	Dust	Rain
Cation to Anion	Slope	0.62	0.24	1.07
	R^2	0.58	0.78	0.97
	Intercept	0.05	0.07	−0.12
$SO_4^{2-}+NO_3^-$ to NH_4^+	Slope	1.11	0.62	1.02
	R^2	0.93	0.87	0.99
	Intercept	−0.07	−0.01	−0.04
$SO_4^{2-}+NO_3^-$ to Ca^2	Slope		1.35	−0.03
	R^2		0.70	0.20
	Intercept		−0.08	0.07

Fig. 8 The same as Fig. 7, but for the electric loads of NH_4^+ and those of SO_4^{2-} plus NO_3^- in different weather processes

weather processes: it was weakly acidic during rainy weather, obviously alkaline during hazy weather and dusty weather, and the alkalinity was significantly stronger during dusty weather.

To further discuss the ionic equilibrium in different weather processes, we analysed the ratios of the main cations to anions in aerosol. First, we detected the relationship between NH_4^+, SO_4^{2-}, and NO_3^- because they are the primary portions of the secondary particles in Guangzhou, which is indicated in Fig. 5 (before the cold air-dust weather period). Figure 6 shows a scatter plot of the electric loads of NH_4^+ and those of SO_4^{2-} plus NO_3^- during different weather processes and their fitting lines (NH_4^+ to SO_4^{2-} plus NO_3^-). During rainy and hazy weather, the fitting linear slopes are both near (slightly larger than) 1, indicating that the electric loads of NH_4^+ are approximately equal to that of the sum of SO_4^{2-} and NO_3^-. Therefore, NH_4^+ is enough to neutralise most of the SO_4^{2-} and NO_3^- during the rainy and hazy weather processes. However, during the cold air-dust weather, the slope is 0.62, obviously below 1, indicating that the electric loads of NH_4^+ are far less than those of the sum of SO_4^{2-} and NO_3^-. Thus, during cold air-dust weather, the amount of NH_4^+ is insufficient to neutralise SO_4^{2-} and NO_3^-, and other important cations should neutralise SO_4^{2-} and NO_3^- (Fig. 8).

Figures 1 and 6 indicate that the Ca^{2+} increased dramatically during the dust-storm period. Thus, we guessed that Ca^{2+} neutralised the SO_4^{2-} and NO_3^-. To confirm this assumption, we analysed the relationship between the electric loads of Ca^{2+} and that of the sum of NO_3^- and SO_4^{2-} in different weather processes. Figure 9 shows their scatter plot and fitting lines (Ca^{2+} to SO_4^{2-} plus NO_3^-). During the cold air-dust weather period, the fitting linear slope is 1.35, indicating that the electric load of Ca^{2+} is more than that of the sum of SO_4^{2-} and NO_3^-. Ca^{2+} is abundant to neutralise most of the SO_4^{2-} and NO_3^- during dusty weather. Meanwhile, during the rainy and hazy weather processes, the fitting linear slopes are near zero, indicating that the combination of SO_4^{2-} and NO_3^- with Ca^{2+} is rare.
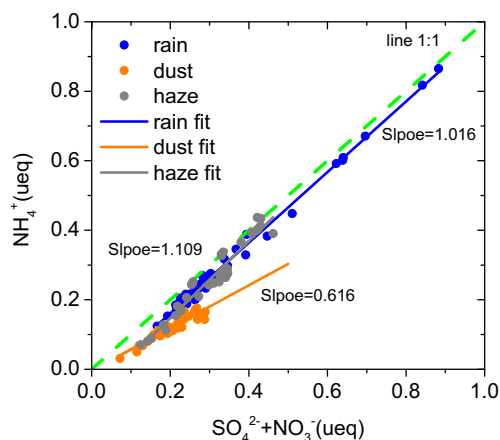
6 Conclusions

During the period from March 16th to 25th, Guangzhou experienced two different weather processes. One was rainy weather from March 16th to 17th, which was characterised by 100 % relative humidity. The other was the intrusion of cold air-dust weather from northern China during the period of March 23rd to 25th, which was characterised by dramatically increased pressure, decreased temperature and increased Ca. Using aerosol data observed hourly by Marga ADI 2080 and Grimm 180, we explored the characteristics of aerosols during different weather processes.

The rainy weather acted as a cleaner to the aerosol through the wet removal effect of rain droplets. The mass concentration of PM and total water-soluble components decreased obviously. The intrusion of cold air-dust weather exhibited both cleaning effect and dust effect. The cleaning effect emerged approximately half a day earlier than the dust effect, and the cleaning effect was drastic whereas the dust effect was gradual. The mass concentration of PM and total water-soluble
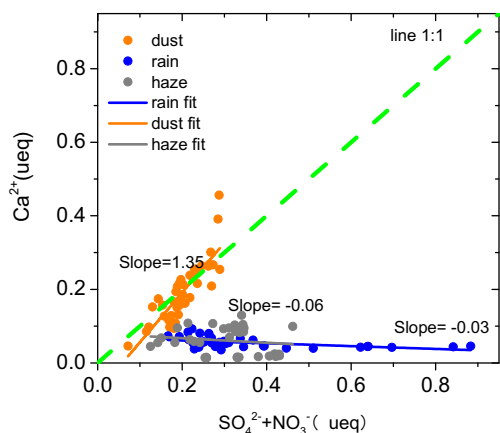
Fig. 9 The same as Fig. 7, but for the electric loads of Ca^{2+} and those of SO_4^{2-} plus NO_3^- in different weather processes

components first dropped dramatically to an abnormally low level and then rose gradually to an abnormally high level. The cold air and dust aerosols from northern China mainly brought in coarse particles that contained a large proportion of Ca^{2+}. As a result, the mass concentration of PM_{10} and Ca^{2+} increased significantly, the ratio of $PM_{2.5}/PM_{10}$ and PM_1/PM_{10} decreased, and the proportion of Ca^{2+} in the total water-soluble components increased to as high as 50 %.

We further analysed the ionic equilibrium in these two weather processes and compared it with that in a typical hazy day during the same period. The cation–anion equilibrium showed a difference in different weather conditions: slightly acidic during rainy weather, and obviously alkaline during hazy weather and cold air-dust weather, with significantly higher alkalinity during cold air-dust weather. Most of the anions, including SO_4^{2-} and NO_3^-, were neutralised by NH_4^+ during the rainy and hazy weather, and by Ca^{2+} during dusty weather.

References

Avol EL, Jones MP, Bailey RM, Chang NM, Kleinman MT, Linn WS, Bell KA, Hackney JD (1979) Controlled exposures of human volunteers to sulfate aerosols. Health effects and aerosol characterization. Am Rev Respir Dis 120(2):319–327

Chate DM, Pranesha TS (2004) Field studies of scavenging of aerosols by rain events. J Aerosols Sci 35:695–706

Chow JC, Watson JG, Kuhns H, Etyemezian V, Lowenthal DH, Crow D, Kohl SD, Engelbrecht JP, Green MC (2004) Source profiles for industrial, mobile, and area sources in the big bend regional aerosol visibility and observational study. Chemosphere 54(2):185–208

Coakley JA Jr, Cess RD, Yurevich FB (1983) The effect of tropospheric aerosols on the earth's radiation budget: a parameterization for climate models. J Atmos Sci 40:116–138

Cowen K, Hanft E, Kelly T, et al (2011) Environmental technology verification report, ETV advanced monitoring systems center. Applikon MARGA semi-continuous ambient air monitoring system

DeLuisi JJ, Furukawa PM, Gillette DA, Schuster BG, Charlson RJ, Porch WM, Weinman JA, Rabinoff RA, Twitty JT (1976) Results of a comprehensive atmospheric aerosol-radiation experiment in the Southwestern United States Part I: size distribution, extinction optical depth and vertical profiles of aerosols suspended in the atmosphere. J Appl Meteorol 15:441–454

Deng T, Deng XJ, Wu D, Tan HB, Li F, Feng YR, Zheng JY, Liao BT (2012) Study on numerical forecast model of haze over Pearl River Delta region and routine business assessment. Adv Meteorol Sci Technol 2:38–44 (in Chinese)

Dockery DW, Schwartz J, Spengler JD (1992) Air pollution and daily mortality: associations with particulates and acid aerosols. Environ Res 59(2):362–373

Fang M, Zheng M, Wang F, Chim KS, Kot SC (1999) The long-range transport of aerosols from northern China to Hong Kong—a multi-technique study. Atmos Environ 33:1803–1817

Flossmann AI, Hall WD, Pruppacher HR (1985) A theoretical study of the wet removal of atmospheric pollutants. Part I: the redistribution of aerosol particles captured through nucleation and impaction scavenging by growing cloud drops. J Atmos Sci 42(6):583–606

Garland JA (1978) Dry and wet removal of sulphur from the atmosphere. Atmos Environ (1967) 12(1):349–362

Gautam R, Hsu NC, Lau KM, Kafatos M (2009) Aerosol and rainfall variability over the Indian monsoon region: distributions, trends and coupling. Ann Geophys 27(9):3691–3703, Copernicus GmbH

Goodwin B, Deojay D, Cowen K, et al (2009) Environmental technology verification report, ETV advanced monitoring systems center. Applikon MARGA semi-continuous ambient air monitoring system

Gu Y, Li HL, Dong Z, Dai T (2009) Study on relation between dust weather and TSP and PM_{10} pollution of Huhhot in 2008 spring. Environ Monit Chin 25:95–98 (in Chinese)

Hales JM (1978) Wet removal of sulfur compounds from the atmosphere. Atmos Environ (1967) 12(1):389–399

Jayaraman A (2001) Aerosol radiation cloud interactions over the tropical Indian Ocean prior to the onset of the summer monsoon[J]. Curr Sci 81(11):1437–1445

Jin M, Shepherd JM (2008) Aerosol relationships to warm season clouds and rainfall at monthly scales over east China: Urban land versus ocean. J Geophys Res: Atmos (1984–2012), 113(D24)

Jinhuan Q, Liquan Y (2000) Variation characteristics of atmospheric aerosol optical depths and visibility in North China during 1980–1994. Atmos Environ 34(4):603–609

Kang HQ, Zhu L, Fan SG (2009) Size distributions and wet scavenging properties of winter aerosol particles in North Suburb of Nanjing. Clim Environ Res 14(5):523–530 (in Chinese)

Kennedy IM (2007) The health effects of combustion-generated aerosols. Proc Combust Inst 31(2):2757–2770

Kim DH, Sohn BJ, Nakajima T, Takamura T (2005) Aerosol radiative forcing over East Asia determined from ground-based solar radiation measurements. J Geophys Res 110(D10):D10S22

Lau KM, Kim KM (2006) Observational relationships between aerosol and Asian monsoon rainfall, and circulation. Geophys Res Lett 33(21)

Lee YL, Sequeira R (2002) Water-soluble aerosol and visibility degradation in Hong Kong during autumn and early winter, 1998. Environ Pollut 116(2):225–233

Li H, Zeng FG, Shao LY, Shi ZB (2002) Current status of study on the human health effects of inhalable particulates. J Environ Health 19: 85–87 (in Chinese)

Li BG, Ran Y, Tao S (2008a) Seasonal variation and spatial distribution of atmospheric aerosols in Beijing. Acta Sci Circumst 28:1425–1429 (in Chinese)

Li F, Wu D, Wang T, Chen J (2008b) Haze weather problems in Guangzhou 2010 Asian Games. Guangdong Meteorol 30:19–21 (in Chinese)

Lin CY, Wang Z, Chen WN, Chang SY, Chou CCK, Sugimoto N, Zhao X (2007) Long-range transport of Asian dust and air pollutions to Taiwan: observed evidence and model simulation. Atmos Chem Phys 7:423–434

Liu TS (1985) Loess and the environment. Beijing: Chin Ocean Press 31: 65

Mircea M, Stefan S, Fuzzi S (2000) Precipitation scavenging coefficient: influence of measured aerosol and raindrop size distribution. Atmos Environ 34:5169–5174

Pöschl U (2005) Atmospheric aerosols: composition, transformation, climate and health effects. Angew Chem Int Ed 44(46):7520–7540

Presto AA, Huff Hartz KE, Donahue NM (2005) Secondary organic aerosol production from terpene ozonolysis. 1. Effect of UV radiation. Environ Sci Technol 39(18):7036–7045

Prospero JM, Ginoux P, Torres O, Nicholson SE, Gill TE (2002) Environmental characterization of global sources of atmospheric soil dust identified with the Nimbus 7 Total Ozone Mapping Spectrometer (TOMS) absorbing aerosol product. Rev Geophys 40(1):2–1

Qiu QH (2004) Influence of sand weather on air quality of Beijing and its forecast. Res Environ Sci 17:56–58 (in Chinese)

Raizenne M (1996) Health effects of acid aerosols on North American children: pulmonary function. Environ Health Perspect 104:506–514

Raizenne ME, Burnett RT, Stern B, Franklin CA, Spengler JD (1989) Acute lung function responses to ambient acid aerosol exposures in children. Environ Health Perspect 79:179

Rogge WF, Hildemann LM, Mazurek MA, Cass GR, Simoneit BR (1993) Sources of fine organic aerosol. 3. Road dust, tire debris, and organometallic brake lining dust: roads as sources and sinks. Environ Sci Technol 27(9):1892–1904

Rotstayn LD, Lohmann U (2002) Tropical rainfall trends and the indirect aerosol effect. J Clim 15(15):2103–2116

Rotstayn LD, Jeffrey SJ, Collier MA, Dravitzki SM, Hirst AC, Syktus JI, Wong KK (2012) Aerosol-and greenhouse gas-induced changes in summer rainfall and circulation in the Australasian region: a study using single-forcing climate simulations. Atmos Chem Phys 12(14):6377–6404

Shen C, Li Y, Wang XM, Huang W, Liang GX, Wang SY, Huang ZE, Chen QJ, Yang LL (2012) Impact of a strong northern dust storm on the air quality in Guangzhou: a case study. Acta Sci Circumst 32:1725–1735 (in Chinese)

Takemura T, Nozawa T, Emori S, Nakajima TY, Nakajima T (2005) Simulation of climate response to aerosol direct and indirect effects with aerosol transport-radiation model. Journal of Geophysical Research: Atmospheres (1984–2012), 110(D2).

Tegen I, Fung I (1995) Contribution to the atmospheric mineral aerosol load from land surface modification. J Geophys Res 100(D9):18707–18718

Thurston GD, Ito K, Hayes CG, Bates DV, Lippmann M (1994) Respiratory hospital admissions and summertime haze air pollution in Toronto, Ontario: consideration of the role of acid aerosols. Environ Res 65(2):271–290

Volkamer R, Jimenez JL, San Martini F, Dzepina K, Zhang Q, Salcedo D, Molina LT, Worsnop DR, Molina MJ (2006) Secondary organic aerosol formation from anthropogenic air pollution: rapid and higher than expected. Geophys Res Lett 33(17):L17811

Wang Y, Zhuang GS, Tang AH, Zhang WJ, Sun YL, Wang ZF, An ZS (2007) The evolution of chemical components of aerosols at five monitoring sites of China during dust storms. Atmos Environ 41:1091–1106

Wendisch M, Keil A, Müller D, Wandinger U, Wendling P, Stifter A, Petzold A, Fiebig M, Leiterer U (2002) Aerosol-radiation interaction in the cloudless atmosphere during LACE 98 1. Measured and calculated broadband solar and spectral surface insolations. J Geophys Res 107(D21):8124

Wu D (2003) A review and outlook on the aerosol study over South China. J Trop Meteorol 19(Suppl):145–151, in Chinese

Wu D, Bi XY, Deng XJ, Li F, Tan HB, Liao GL, Huang J (2006a) Effect of atmospheric haze on the deterioration of visibility over the Pearl River Delta. Acta Meteorol Sin 64:510–517 (in Chinese)

Wu D, Bi XY, Deng XJ, Pan WJ, Huang J (2006b) Heavy haze weather resulting from aerosol cloud over Pearl River Delta. J Nat Disasters 15:77–83 (in Chinese)

Wu D, Li F, Deng XJ, Bi XY, Wang XH, Huang XY (2009) Study on the chemical characteristics of polluting fog in Guangzhou area in spring. J Trop Meteorol 15(1):68–72

Wu D, Wu C, Li HY, Chen HH, Deng T (2011) Dusty sky in Hong Kong and clear sky in the inland of the Pearl River Delta: analysis of a typical haze episode during 17–23 March 2010. Acta Sci Circumst 31:695–703 (in Chinese)

Xia D, Yang SJ, Wu D, Hu ST, Li F, He XC, Tan HB, Deng XJ, Bi XY, Fan SJ (2009) Analysis of the mass spectrum and water dissoluble components of atmospheric aerosols over Guangzhou. J Trop Meteorol 25:675–680 (in Chinese)

Zhang LM, Michelangeli DV, Taylor PA (2004) Numerical studies of aerosol scavenging by low-level, warm stratiform clouds and precipitation. Atmos Environ 38:4653–4665

Zhao HB, Zheng CG (2006) Stochastic algorithm and numerical simulation for drop scavenging of aerosols. Appl Math Mech 27:1159–1168 (in Chinese)

Zhi YH, Fu C, Shao ZH (2007) The dust weather and its influence on air quality in Lanzhou city. J Catastrophol 22:77–80 (in Chinese)